

Charge transfer in slow collisions of C^{6+} with H below 1 keV/amu

Chien-Nan Liu,¹ Shu-Chun Cheng,² Anh-Thu Le,² and C. D. Lin²

¹*Department of Physics, Fu-Jen Catholic University, Taipei 24205, Taiwan*

²*Department of Physics, Kansas State University, Manhattan, Kansas 66506, USA*

(Received 13 March 2005; published 26 July 2005)

We reexamine the charge transfer cross sections for $C^{6+}+H$ collisions for energies below 1 keV/amu using a fully quantum mechanical approach, based on the hyperspherical close-coupling method. Whereas most previous theoretical and experimental data agree well for the dominant charge transfer to the $C^{5+}(n=4)$ states, there is significant disagreement among the theories for the transition to the weaker $n=5$ states. Using the present quantum mechanical calculations we analyze the origin of the discrepancy among these previous calculations. We further extend the calculations to collision energies down to about 1 eV and show that electron capture to the $n=5$ states begins to dominate over the $n=4$ states.

DOI: [10.1103/PhysRevA.72.012717](https://doi.org/10.1103/PhysRevA.72.012717)

PACS number(s): 34.70.+e, 31.15.Ja

I. INTRODUCTION

Charge transfer processes in slow ion-atom collisions are examples of rearrangement processes that are challenging both theoretically and experimentally [1]. Traditional approaches are based on semiclassical close-coupling formalism within which electronic transitions occur via nonadiabatic couplings and nuclear motion is treated classically [2]. Different methods employ either atomic orbital (AO) or molecular orbital (MO) basis expansions. As the collision energy decreases, the semiclassical method needs to be modified to account for the trajectory effects of the nuclear motion. However, the effective interaction potential between the two heavy nuclei is not uniquely defined. In practice, in some calculations curved trajectories are used, while in others trajectories are straight lines. Clearly, at low energies, a fully quantum mechanical treatment for both the electronic and nuclear motion is necessary in order to avoid the ambiguities associated with trajectory effects.

Several theoretical studies, based on either AO or MO expansions, on charge transfer cross sections for slow $C^{6+}+H$ collisions have been carried out since the early 1980s. While results from most calculations agree on the cross sections for charge transfer into the dominant $n=4$ channels, predictions for the weaker $n=5$ cross sections vary substantially. Thus the recent theoretical studies has focussed primarily on the cross sections for transfer into the $C^{5+}(n=5)$ channels. Among the theoretical calculations, Green *et al.* [3] performed semiclassical MO calculations using a basis spanning the $C^{5+}(n=3-6)$ manifolds and curved trajectories based on average molecular potential. Other semiclassical MO calculations were carried out by Harel *et al.* [4] using all states converging to $C^{5+}(n=1-8)$ thresholds and straight-line trajectories. These two semiclassical MO calculations achieve good agreement in the high energy region, but their predictions for the $n=5$ cross sections deviate at energies below 700 eV/amu. Calculations of Fritsch and Lin [5] was based on AO expansion with a basis spanning the $C^{5+}(n=4$ and 5) manifolds and unscreened Coulomb trajectories. However, predictions from early AO calculations start to deviate from those MO results at collision energies around

5 keV/amu and the difference exceeds one order of magnitude around 100 eV/amu.

Recently, Caillat *et al.* [6] carried out an extensive study on this system using close-coupling method with a much larger AO basis set for collision energies above 50 eV/amu. They performed calculations using different basis sets and various choices of trajectories. With the larger basis set, their results for the $n=5$ cross sections agree with the calculations using MO basis [3,4] above about 500 eV/amu, thus establishing that the lower cross sections predicted by Fritsch and Lin [5] and Kimura and Lin [7], are due to the insufficient basis set used in their respective calculations. Their results obtained from straight-line trajectory approximation deviate from those MO results, predicting higher values for the $C^{5+}(n=5)$ cross sections in the energy region below 200 eV/amu. To account for the effects of curved trajectories, they used a model to fold the straight-line coupled-channel results with deflection functions obtained by classical trajectory Monte Carlo (CTMC) calculations. Such procedure results in a reduction of the $n=5$ cross sections at low energies and brings the values of their prediction almost identical to those of Harel *et al.* [4], but still higher than those of Green *et al.* [3].

In this paper, we employ a fully quantum mechanical approach, instead of the semiclassical approach, such that there is no need to make assumptions on the trajectories. To eliminate the additional ambiguity of introducing electron translational factor or reaction coordinates [8,9], we based the calculation on the recently developed hyperspherical close-coupling (HSCC) method [10]. The HSCC method is formulated similarly to the perturbed stationary states (PSS) approximation but without the well-known difficulties of that approach. No additional assumptions are needed beyond the truncation of the number of channels included in the calculations. Also, since it is fully quantum mechanical, trajectories of the nuclear motion are irrelevant. Therefore, the HSCC approach can be used to evaluate the results from various semiclassical calculations at the low energies. Detailed comparison between results from the present calculation and previous works will be presented, shedding light on the limitations of various approaches, particularly the effects

of trajectory in semiclassical approximations. Atomic units are used unless otherwise indicated.

II. THEORY

We employ the hyperspherical close-coupling method recently developed by Liu *et al.* [10]. The HSCC has proved successful in previous applications [10–12] to ion-atom collisions involving systems with one electron and two heavy nuclei (or positive ions with closed shell electrons). This method has been described in detail in Ref. [10]. Thus we present here only a brief overview of the HSCC method.

The three-body collision complex, CH^{6+} , is described by mass-weighted hyperspherical coordinates. In the “molecular” frame, the first Jacobi vector $\boldsymbol{\rho}_1$ is chosen to be the vector from C^{6+} to H^+ , with a reduced mass μ_1 . The second Jacobi vector $\boldsymbol{\rho}_2$ goes from the center of mass of C^{6+} and H^+ to the electron, with a reduced mass μ_2 . The hyperradius R and the hyperangle ϕ are defined as

$$R = \sqrt{\frac{\mu_1}{\mu} \rho_1^2 + \frac{\mu_2}{\mu} \rho_2^2}, \quad (1)$$

$$\tan \phi = \sqrt{\frac{\mu_2 \rho_2}{\mu_1 \rho_1}}, \quad (2)$$

where μ is arbitrary. Another angle, θ , is defined as the angle between the two Jacobi vectors. When μ is chosen equal to μ_1 , the hyperradius R is very close to the internuclear distance between C^{6+} and H^+ .

We first introduce the rescaled wave function

$$\Psi(R, \Omega, \hat{\omega}) = \psi(R, \Omega, \hat{\omega}) R^{3/2} \sin \phi \cos \phi, \quad (3)$$

then the Schrödinger equation takes the form

$$\left(-\frac{1}{2} \frac{\partial}{\partial R} R^2 \frac{\partial}{\partial R} + \frac{15}{8} + H_{\text{ad}}(R; \Omega, \hat{\omega}) - \mu R^2 E \right) \Psi(R, \Omega, \hat{\omega}) = 0, \quad (4)$$

where $\Omega \equiv \{\phi, \theta\}$, and $\hat{\omega}$ denotes the three Euler angles of the body-fixed frame with respect to the space-fixed frame. H_{ad} is the adiabatic Hamiltonian,

$$H_{\text{ad}}(R; \Omega, \hat{\omega}) = \frac{\Lambda^2}{2} + \mu R C(\Omega), \quad (5)$$

where Λ^2 is the square of the grand angular momentum operator and $C(\Omega)/R$ gives the total Coulomb interaction.

To solve Eq. (5), we expand the rescaled wave function in terms of normalized and symmetrized rotation function \tilde{D} , and body-frame adiabatic basis functions $\Phi_{\nu l}(R, \Omega)$,

$$\Psi(R, \Omega, \hat{\omega}) = \sum_{\nu} \sum_I F_{\nu l}(R) \Phi_{\nu l}(R, \Omega) \tilde{D}_{IM_J}^J(\hat{\omega}), \quad (6)$$

where ν is the channel index, J is the total angular momentum, I is the absolute value of the projection of \mathbf{J} along the body-fixed z' axis and M_J is the projection along the space-fixed z axis. $\Phi_{\nu l}$ are eigenfunctions of a reduced adiabatic Hamiltonian which does not include any J -dependent terms.

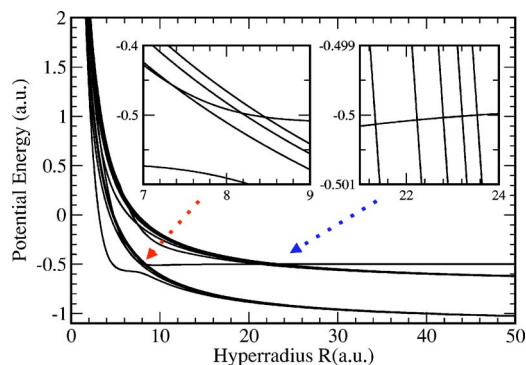


FIG. 1. (Color online) Hyperspherical potential curves for CH^{6+} . This figure shows only the $I=0$ channels. The insets show areas with complicated avoided crossings in more detail.

In practice, it is more efficient to diabaticize the potential curves and then use the diabatic basis set in the expansion (6). This modification of the HSCC, usually called the diabatic HSCC, has been introduced by Hesse *et al.* [13]. A nice feature of this modification is that it allows us to conveniently discard channels that are weakly coupled to the main channels [14,15]. In this paper we used both adiabatic and diabatic expansions and found excellent agreements between them.

To solve the hyperradial equations we divided the hyper-radial space into sectors. We then used a combination of the R -matrix propagation method [16] to propagate the R -matrix from one sector to the next, and a slow/smooth-variable discretization method [17] within each sector. Note that both radial and rotational couplings are fully incorporated. The R -matrix is propagated to a large hyperradius (depending on the collision energy) where the solution is matched to the known asymptotic solutions to extract the scattering matrix. The electron capture cross section for each partial wave J is then obtained from the calculated scattering matrix.

The method described above must be carried out for each partial wave J until a converged cross section is reached. Using the numerical procedure introduced in Liu *et al.* [10] such calculations can be easily carried out for many partial waves. We have checked that the results are insensitive to the matching radius within the number of channels included in the calculation.

III. RESULTS AND DISCUSSION

The hyperspherical potential curves included in the calculation for R up to 50 a.u. are presented in Fig. 1. For clarity, only $I=0$ components are shown. Note that, these channels are not exact adiabatic channels since they are obtained by diagonalizing the reduced electronic Hamiltonian for each I . In order to achieve convergence in the energy region considered, we include all the $I=0, 1$, and 2 channels converging to $\text{C}^{5+}(n=4)+\text{H}^+$ and $\text{C}^{5+}(n=5)+\text{H}^+$ thresholds, in addition to the initial $\text{C}^{6+}+\text{H}(1s)$ channel. Note that rotational coupling terms are incorporated in the current implementation of the HSCC method. As a result, there are 23 coupled channels in the present full calculation. For the low energy regime fewer

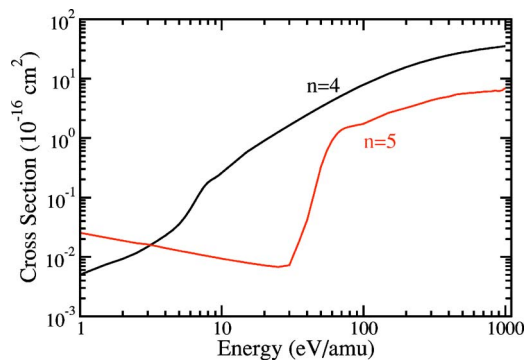


FIG. 2. (Color online) Present results for the charge transfer cross sections for the processes $C^{6+} + H(1s) \rightarrow C^{5+}(n=4,5) + H^+$.

channels are already adequate. These potential curves and the numerous avoided crossings are instrumental in understanding how transitions, charge transfer in this case, occur.

These potential curves show three regions where pronounced avoided crossings can be observed. The outermost avoided crossings between the incoming channel and the $n=5$ manifold are very narrow and are located at around $R=22$ a.u. These crossings can be treated diabatically except at very low collision energies. The next region of avoided crossings occurs near $R=8$ a.u., where the entrance channel interacts strongly with the $C^{5+}(n=4)$ manifold. The third region of avoided crossings occur at much smaller R , near about $R=1.5$ a.u. (see Fig. 3), where the channels converging to the $C^{5+}(n=5)$ threshold, as well as the entrance channel, interact efficiently. We will point out that this innermost avoided crossing region, which is difficult to be accounted for accurately by expansions using atomic basis functions, is responsible for the discrepancy of the $n=5$ cross sections among the different theories.

In Fig. 2, we first present the charge transfer cross sections for $C^{6+} + H(1s)$ collisions at energies from 1 eV/amu up to 1 keV/amu obtained from the present HSCC calculation. As expected, the $n=4$ channels are dominant for energies above 4 eV/amu. While the $n=4$ cross section increases smoothly as the collision energy increases, the $n=5$ cross section exhibits interesting energy dependence, including a sharp drop below 70 eV/amu and a steady increase below 30 eV/amu. Such energy dependence can be understood in terms of the avoided crossings of potential curves in Fig. 1.

We first take a closer look of the avoided crossings near $R=8$ a.u. Using the diabaticization procedure described earlier, the complicated adiabatic potential curves of Fig. 1 below $R=10$ a.u. are shown as diabatic curves in Fig. 3. Here we plot the “electronic” part of the diabatic curves, obtained by subtracting the internuclear Coulomb potential energy $6/R$ at each R ; again only the $l=0$ curves are shown. [Recall that for $R \geq 1$ a.u. the hyperradius and the internuclear distance are essentially identical since we choose $\mu = \mu_1$, see Eq. (1)]. With this set of diabatic curves, we note that the entrance channel still shows strong avoided crossing with the lowest $n=4$ channel. The entrance channel also interacts conspicuously with the $n=5$ channels near $R=1.5$ a.u. We will use Fig. 3, together with Fig. 1, to explain the calculated energy dependence of the $n=4$ and $n=5$ charge transfer cross sections shown in Fig. 2.

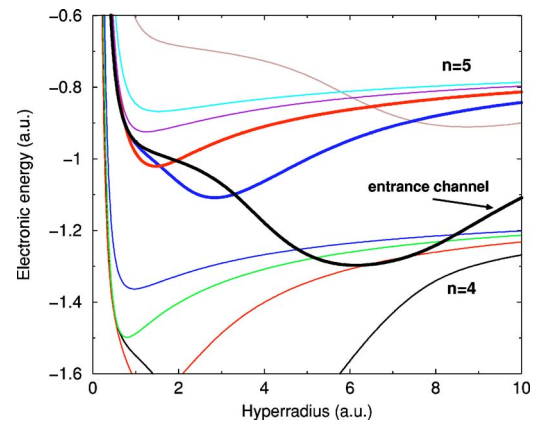


FIG. 3. (Color online) “Electronic” part of the hyperspherical potential curves for CH^{6+} . Note that the curves have been diabaticized. See text for more details.

To begin with, let us examine the energy region from 100 eV/amu to 1000 eV/amu. At such high energies, the avoided crossings between the entrance channel and the $n=5$ states near $R=22$ a.u. can be treated diabatically. Thus the entrance channel directly enters the region near $R=8$ a.u. (see Fig. 3) where it can interact efficiently with the lowest $n=4$ channel. This strong avoided crossing is responsible mostly for populating the $n=4$ channels.

In Fig. 4 we compare our calculations with previous theoretical results for this system. It is clear that all the theoretical calculations agree on the $n=4$ cross sections, whether the calculations were carried out using AO or MO basis functions.

How about the $n=5$ cross sections? In this case the earlier calculations based on the AO’s [5,7] are distinctly much lower than those based on the MO’s, although the newer AO calculations by Caillat *et al.* [6], by using a much larger AO basis, were able to obtain $n=5$ cross sections in better agree-

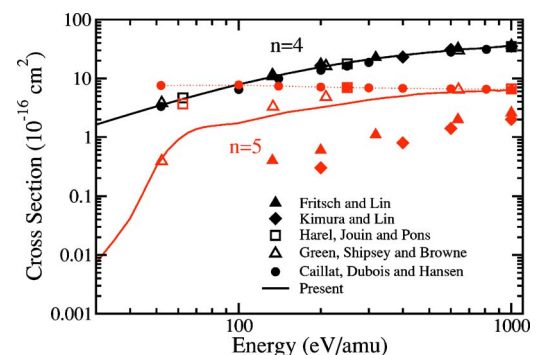


FIG. 4. (Color online) Comparison of calculated total charge transfer cross sections for $C^{6+} + H(1s) \rightarrow C^{5+}(n=4,5) + H^+$. Present results are shown in solid lines. Other theoretical predictions are shown in symbols. Both the results of Caillat *et al.* [6] and those of Kimura and Lin [7] are obtained from AO calculations with straight-line trajectories. Results of Harel *et al.* [4] are calculated using MO basis and straight-line trajectories. Results of Green *et al.* [3] are obtained from MO calculations using curved trajectories. The dotted line connecting the results of Caillat *et al.* indicates an energy dependence different from others.

ment with calculations using MO's, see Fig. 4. We have repeated their calculations with the larger AO basis set and obtained identical results. Thus the earlier small $n=5$ cross sections using AO basis sets [5,7] can be explained as due to the "lack of convergence" in the AO calculation. We note that similar discrepancy has been found between the AO and MO calculations for the weaker $n=6$ channels in $O^{8+}+H$ collisions and the discrepancy has been resolved by recent HSCC calculations [14]. (The comment made in this paper was incorrect. The discrepancy in the previous AO calculations was not due to computer program errors using curved trajectories, but rather due to the basis set used was too small.)

In Fig. 4 we note that the AO results for the $n=5$ cross sections from Caillat *et al.* appear to increase slowly with decreasing energies, while the MO results appear to decrease with decreasing energies. Our present HSCC results agree well with those obtained by Green *et al.* [3], who employed a semiclassical MO formalism with a basis set spanning the $C^{5+}(n=3-6)$ manifolds and curved trajectories based on average molecular potential. Also included are results from Harel *et al.* [4], who used a semiclassical MO method with all the states converging to the $C^{5+}(n=1-8)$ thresholds and straight-line trajectories. The predicted values of Harel *et al.* are slightly higher than the present results, but show a similar energy dependence. Note that these two MO calculations begin to deviate at energies lower than 700 eV/amu. In the semiclassical calculations when the trajectory effect becomes important, it is difficult to establish what kind of trajectories is more suitable. In our full quantal HSCC calculations such ambiguity does not exist and our results indicate that the calculations of Green *et al.* [3] appear to be more accurate.

We can understand the results of these different theoretical calculations for the $n=5$ states based on the potential curves detailed in Fig. 3. Since the outer crossings near $R=22$ a.u. are diabatic, the only way the $n=5$ states can be populated is through the avoided crossings near $R=2$ a.u. This is demonstrated by displaying the impact parameter dependence of electron capture probabilities. In Fig. 5 we show the comparison of the results from HSCC with those from the AO calculations (i.e., with a larger basis set, similar to those by Caillat *et al.*) at collision energy of 500 eV/amu and the results agree quite well. Clearly the $n=4$ cross sections are populated at larger impact parameters, extending up to the region of the avoided crossing near $R=8$ a.u. For the $n=5$ cross sections, they are populated at much smaller impact parameters, clearly indicating the importance of avoided crossings near $R=2$ a.u. In general, the crossings or the molecular potential curves at such small internuclear distances are more difficult to obtain accurately using AO as basis, especially if the basis set is too small. This explains why the earlier AO calculations [5,7] gave the incorrect $n=5$ cross sections.

We next set to explain the larger discrepancy between the MO results (and our HSCC results) and the AO calculations of Caillat *et al.* at energies, say, below 200 eV/amu. To highlight the origin of the discrepancy, we compare in Fig. 6 the impact parameter dependence of electron capture probabilities at 50 eV/amu. In this case, the AO and the HSCC results for $n=4$ still agree well, even though the phase of the oscillations in the probability differs. For the $n=5$ states, the AO results are much too large. Note that the HSCC results show cross sections coming from much smaller R . At such low energies the transition probabilities depend critically on the precise avoided crossings and the potential curves in the small- R region, which are difficult to be calculated accurately using the AO basis set. Clearly, the cross sections at small impact parameters are strongly overestimated by the AO calculations, indicating the importance of the trajectory effects at this low energy.

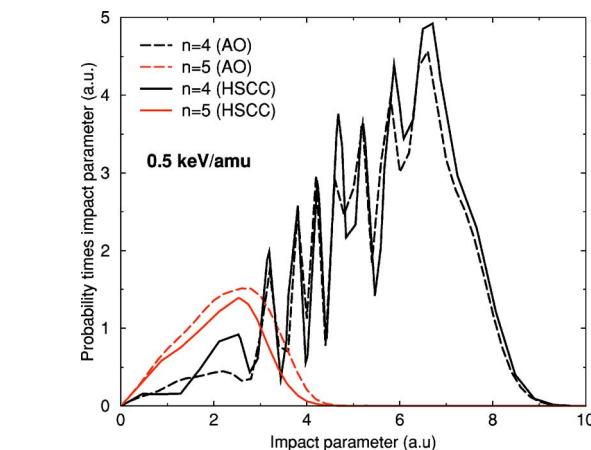


FIG. 5. (Color online) Comparison of the quantal HSCC and semiclassical straight-line trajectory AO results for the impact parameter weighted probability as a function of impact parameter at $E=0.5$ keV/amu.

As one proceeds to lower energies, as can be seen from Fig. 2, the cross section for the $n=5$ states drops precipitously—by more than two orders of magnitude—for energies between 70 eV/amu and 30 eV/amu. This is a consequence of the avoided crossings near $R=1.5$ a.u. for populating the $n=5$ channels (see Figs. 1 and 3). Below about 70 eV/amu, these avoided crossings are energetically inaccessible, in other words, the nuclear wave packet following the entrance channel cannot penetrate the avoided crossing region near $R=1.5$ a.u. except by tunnelling. This would

As one proceeds to lower energies, as can be seen from Fig. 2, the cross section for the $n=5$ states drops precipitously—by more than two orders of magnitude—for energies between 70 eV/amu and 30 eV/amu. This is a consequence of the avoided crossings near $R=1.5$ a.u. for populating the $n=5$ channels (see Figs. 1 and 3). Below about 70 eV/amu, these avoided crossings are energetically inaccessible, in other words, the nuclear wave packet following the entrance channel cannot penetrate the avoided crossing region near $R=1.5$ a.u. except by tunnelling. This would

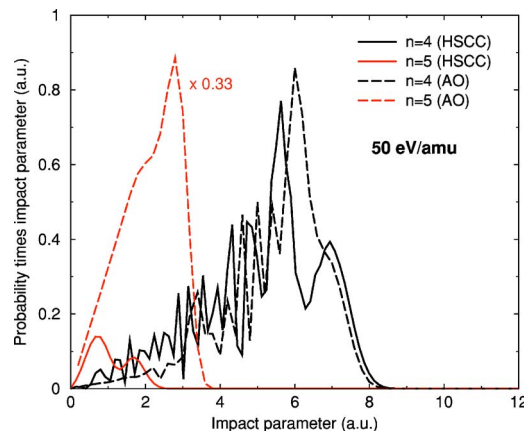


FIG. 6. (Color online) Same as Fig. 5, but for $E=50$ eV/amu. Note that the AO results for the transition to $C^{5+}(n=5)$ have been scaled down by a factor of 1/3.

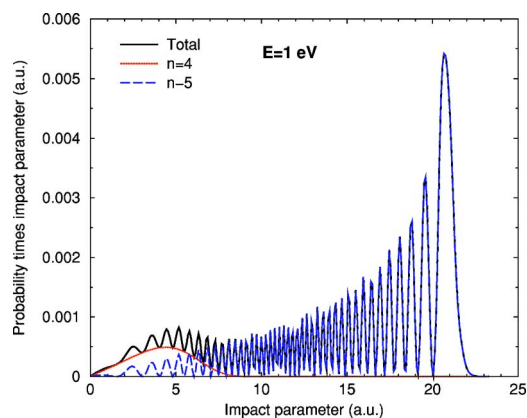


FIG. 7. (Color online) Impact parameter weighted probability as a function of impact parameter at $E=1$ eV.

explain the near exponential decrease of the $n=5$ charge transfer cross section in this energy region.

As the collision energy is further decreased, transition to $n=5$ through the $R=1.5$ a.u. avoided crossing region would become inefficient. However, the outermost avoided crossings near $R=22$ a.u. become less diabatic and direct transitions to the $n=5$ states become possible. In Fig. 7 we show the impact parameter weighted charge transfer probabilities at 1 eV. Note that the $n=5$ probabilities are much larger, and charge transfer occurs at very large impact parameters, extending to impact parameters near 22 a.u. In contrast, charge transfer to the $n=4$ becomes less likely since the avoided crossing near $R=8$ a.u. becomes more and more adiabatic. From Fig. 2 our calculation shows that $n=5$ cross section overtakes $n=4$ at 3 eV/amu.

At energies below about 10 eV/amu, the total as well as charge transfer to the $n=5$ states cross sections have an energy dependence which is consistent with the predictions of the Langevin model [18]. This classical model predicts that the cross section at low energies for ions colliding with a neutral atom or molecule follows

$$\sigma = \pi q \sqrt{\frac{\alpha}{E}}, \quad (7)$$

where q is the charge of C⁶⁺, α is the polarizability of H(1s), and E is the collision energy. Note that the Langevin model

considers the incident trajectories as orbits of an attractive polarization potential,

$$V(r) = -\alpha/2r^4. \quad (8)$$

Such behavior has been predicted in various collision systems with similar long-ranged avoided crossings [12,14,19].

IV. CONCLUSIONS

We have presented fully quantum mechanical calculations using the recently developed HSCC method for the electron-capture cross section for C⁶⁺+H collisions in the energy range from 1 eV/amu to 1 keV/amu. Main dynamical features of this collision system are fully understood with the help of avoided crossings observed in the adiabatic potential curves. Our calculations resolve the discrepancies for the $n=5$ states among the earlier theoretical results. We concluded that the avoided crossings near $R=1.5$ a.u. are the main mechanism for populating the $n=5$ excited states. A good description using AO basis set for this small R region is difficult and this explains the errors of earlier AO-based calculations. We have shown that the trajectory effects need to be included in both semiclassical AO and MO approaches, although it remains ambiguous how this can be done properly. Our results also show strong energy dependence in the $n=5$ cross section at low energies, and the gradual emergence of the Langevin limit behavior at energies below about 10 eV/amu. With the present results, we believe that the discrepancies among the different theoretical results are now resolved, and the cross sections presented in this paper are expected to be quite accurate despite that measurements in the low energy region are not available.

ACKNOWLEDGMENTS

One of the authors (C.N.L.) acknowledges support from the National Science Council of Taiwan, under Grant No. NSC 93-2112-M-030-005. This work was also supported in part by Chemical Sciences, Geosciences and Biosciences Division, Office of Basic Energy Sciences, Office of Sciences, U.S. Department of Energy.

-
- [1] B. H. Bransden and M. R. C. McDowell, *Charge Exchange and Theory of Ion-Atom Collisions* (Clarendon, Oxford, 1992).
- [2] W. Fritsch and C. D. Lin, Phys. Rep. **202**, 1 (1991).
- [3] T. A. Green, M. E. Riley, E. J. Shipsey, and J. C. Browne, Phys. Rev. A **26**, 3668 (1982); T. A. Green, E. J. Shipsey, and J. C. Browne, *ibid.* **25**, 1364 (1982).
- [4] C. Harel, H. Jouin, and B. Pons, At. Data Nucl. Data Tables **68**, 279 (1998).
- [5] W. Fritsch and C. D. Lin, Phys. Rev. A **29**, 3039 (1984).
- [6] J. Caillat, A. Dubois, and J. P. Hansen, J. Phys. B **33**, L715 (2000).
- [7] M. Kimura and C. D. Lin, Phys. Rev. A **32**, 1357 (1985).
- [8] J. B. Delos, Rev. Mod. Phys. **53**, 287 (1981).
- [9] A. T. Le, C. D. Lin, L. F. Errea, L. Mendez, A. Riera, and B. Pons, Phys. Rev. A **69**, 062703 (2004).
- [10] C. N. Liu, A. T. Le, T. Morishita, B. D. Esry, and C. D. Lin, Phys. Rev. A **67**, 052705 (2003).
- [11] A. T. Le, C. N. Liu, and C. D. Lin, Phys. Rev. A **68**, 012705 (2003).
- [12] A. T. Le, M. Hesse, T. G. Lee, and C. D. Lin, J. Phys. B **36**, 3281 (2003).
- [13] M. Hesse, A. T. Le, and C. D. Lin, Phys. Rev. A **69**, 052712 (2004).

- [14] T. G. Lee, M. Hesse, A. T. Le, and C. D. Lin, Phys. Rev. A **70**, 012702 (2004).
- [15] A. T. Le and C. D. Lin, Phys. Rev. A **71**, 022507 (2005).
- [16] D. Kato and S. Watanabe, Phys. Rev. A **56**, 3687 (1995).
- [17] O. I. Tolstikhin, S. Watanabe, and M. Matzuzawa, J. Phys. B **29**, L389 (1996).
- [18] G. Gioumousis and D. P. Stevenson, J. Chem. Phys. **29**, 294 (1958).
- [19] C. N. Liu, A. T. Le, and C. D. Lin, Phys. Rev. A **68**, 062702 (2003).